Draft version January 29, 2025
Typeset using LaTeX twocolumn style in AASTeX631

Not too hot, not too cold: even "Goldilocks" dust temperatures struggle to reconcile implied reddening with IR limits in the brightest Little Red Dots

David J. Setton,[1,*] UNCOVER, and RUBIES

[1] Department of Astrophysical Sciences, Princeton University, 4 Ivy Lane, Princeton, NJ 08544, USA

ABSTRACT

Compact, JWST-discovered Little Red Dots host highly luminous Hα and red rest-optical spectral energy distributions (SEDs), implying that they are powered by some combination of highly attenuated dusty starbursts or active galactic nuclei. However, the lack of any appreciable FIR emission has proved difficult to reconcile with the implied attenuated luminosity in these models. Here, we utilize archival Herschel imaging, new and existing MIRI imaging, and deep new ALMA imaging of the two optically brightest Little Red Dots to place the strongest constraints on the IR luminosity in Little Red Dots to date. The flat rest ~ 4 μm detections rule out any significant energy contribution from hot ($T \gtrsim 500$ K) dust, and the FIR non-detections similarly imply that there cannot be any appreciable cold ($T \lesssim 75$ K) dust component. Together, these constraints essentially rule out the possibility of these LRDs being highly reddened starbursts; not only is their no room in the FIR SED for the reprocessed attenuated light, the systems are also not detected in [CII], implying a non-star forming origin for the highly luminous Hα. Reddened quasar models also predict significant FIR output, and are difficult to square with the total lack of allowance for any hot dust contribution. Finally, composite AGN and galaxy models can fit within our FIR constraints, but only for a very specific dust temperature configuration. We conclude that it is unlikely that LRDs are highly reddened intrinsically blue sources with IR SEDs that conspire to avoid current observing facilities; instead, we propose that these systems may indeed be significantly redder than most models assume, alleviating the need for strong attenuation.

1. INTRODUCTION

- LRDs are weird, highly numerous V-shaped SEDs with broad lines. Coming up with a model that simultaneously can explain the V-shape and the lines is a bit of a white whale of early JWST.

- On the one hand, the present of Balmer breaks makes it seem like these things must have some kind of galaxy component. Models that attempt to reproduce the full SED with starlight only invariably result in dusty, highly star forming systems. Broad lines here can be attributed to highly compact sizes (Baggen et al. 2023, 2024), and the V-shape to the intersection of the dusty starburst and some leaking UV. These models have a number of problems, namely the high stellar densities that are unprecedented.

- On the other hand, an AGN interpretation seems more natural given that these things are point sources with broad lines. Some outstanding issues with this model are the lack of x-rays (though this can potentially be resolved with super-eddington accretion) and the lack of a natural explanation for the Balmer location of the "V". Recently, it has been proposed that an accretion disk buried in dense gas could help by making the intrinsic disk have a break (Inayoshi & Maiolino 2024; Ji et al. 2025).

- Additionally, people have fit composite models that combine these components, but all models share the same feature: you are taking an extremely blue intrinsic SED and reddening it to match the observed continuum shape. These models have a problem, given that LRDs show no evidence of either hot or cold dust, even in stacks (Labbé et al. 2023; Williams et al. 2024; Casey et al. 2024; Akins et al. 2024). There have been attempts to model around this by invoking specific dust temperature distributions that can skirt existing constraints (Li et al. 2024), but at the end of the day it's hard to square a reddened AGN or starburst not having any appreciable FIR emission.

* Email: davidsetton@princeton.edu
Brinson Prize Fellow

- One of the biggest issues of constraints of the dust SED in LRDs have been that the sources themselves aren't intrinsically that bright, which has forced us to resort to stacking. However, the most optically luminous LRDs present the best chance at getting meaningful constraints on an individual object basis.

- Here, we present a full SED analysis of two of the optically luminous LRDs, A2744-45924 (Labbe et al. 2024) and RUBIES-BLAGN-1 (Wang et al. 2024a), including newly obtained deep ALMA drills and new MIRI observations for A2744-45924. The goal of this letter is not to present a fully consistent model of the SED with these new limits. Rather, we perform a simple exercise of measuring the maximum IR luminosity and dust SED shape that our full SED constraints can tolerate, and comparing those constraints to commonly assumed models of LRDs.

- Paper is laid out as follows blah blah blah

2. DATA

2.1. *The two most Hα luminous LRDs to date*

2.1.1. *Rest-UV and Optical Data*

2.1.2. *Models*

While the specifics of fitting LRD models vary in the literature as the field grapples with these novel SED shapes, essentially all models that can successfully reproduce the spectral energy distribution of these "V-shaped" sources in detail invoke an intrinsically blue galaxy, AGN, or composite with some kind of break at 0.3645 μm and selectively redden it to match the observed weak UV, red continuum, and strong lines. Under the assumption of energy balance, the strong attenuated UV predicts a high FIR luminosity.

In this work, we directly utilize the best fitting models for A2744-45924 and RUBIES-BLAGN-1 from Labbe et al. (2024) and Wang et al. (2024a). We refer the reader to Labbe et al. (2024) and Wang et al. (2024a) for the specific ingredients of each of these models, but in practice, they both work similarly in that they assume a range of stellar populations (via non-parametric star formation histories or a delayed-tau model) and intrinsic AGN SEDs that experience varying levels of reddening that together can produce the full SED. (**do we need more detail than this?**) In particular, we directly utilize their predictions for the attenuated luminosity (which agree between models and sources within a factor of ~ 0.5 dex) to motivate the acquisition of mid- and far-IR data, hoping to validate their models (via detection of a bright dust SED) or to cast doubt on either the assumption of energy balance or the intrinsic SED shape. As both the sources in this study exhibit strong Balmer breaks, we specifically focus on two classes of models in their works: galaxy only fits and galaxy+AGN composites, which were required in both works to produce these observed break features. We acknowledge that a separate class of models where an AGN is embedded dense, hot gas has also been shown to be able to create a similar break (Inayoshi & Maiolino 2024; Ji et al. 2025); however, we will argue that the intrinsic SED predicted by those works that is still subjected to intense reddening is qualitatively similar to the composite models we employ here, resulting in similar conclusions as they relate to energy balance.

To demonstrate the level of reddening that these classes of models assume, in Figure 1 we show the best fitting composite model from Labbe et al. (2024) without any dust attenuation (blue), as well as the observed spectrum (goldenrod). This specific model predicts a total attenuated luminosity $\sim 1.8 \times 10^{12} L_\odot$, with $\sim 90\%$ of that luminosity produced by the AGN component and the remaining 10% coming from a reddened post-starburst galaxy that produces the break and contributes to the red continuum. The predicted attenuated luminosity for the composite model in Wang et al. (2024a) is almost identical at $\sim 3 \times 10^{12} L_\odot$, though in contrast the AGN contribution in this case is almost 100% because the galaxy component in their model covers the UV optical rather than the red end. **Maybe a statement about how powerful this approach is precisely because all the predicted luminosities are so close to one another.**

If the dust covering fraction is near unity, this entire budget of attenuated luminosity should be re-emitted in a dust SED that peaks somewhere in the mid/far-IR, depending on the dust temperature. In the next section, we utilize this as motivation for our follow-up observations to constrain this predicted dust distribution across a wide range of assumed temperature.

2.2. *IR Constraints*

Given that models make clear predictions for the IR luminosity but are agnostic to the specific SED shape of that emission, we conduct a wide search for this IR luminosity across the entire IR SED that is accessible to our current observing facilities. In this section, we outline our motivation for each IR data source, as well as our observing strategy in reductions when new data was taken.

2.2.1. *MIRI*

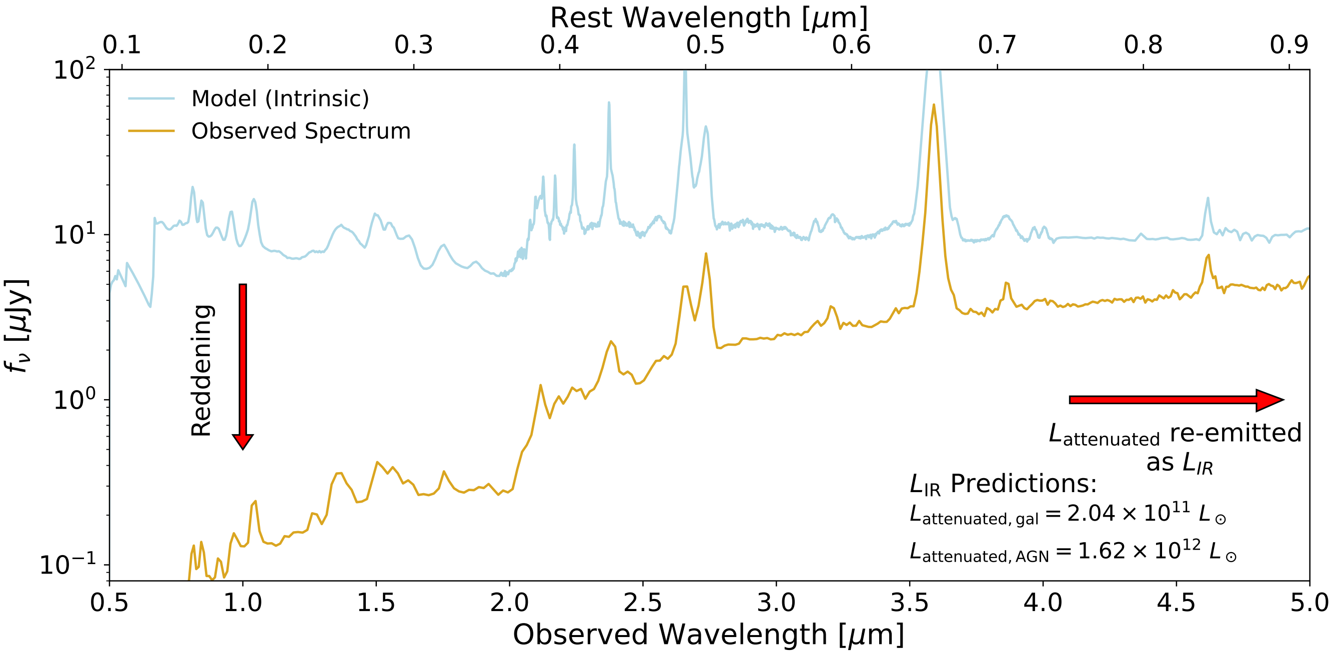

Figure 1. A demonstration of the fundamental assumption that goes into the vast majority of LRD models, using the composite model from Labbe et al. (2024) for A2744-45924. In blue, we show the intrinsic, unattenuated galaxy+AGN model, which, via a combination of reddening and scattering, is observed in the rest optical as the NIRSPEC/PRISM spectrum (orange). The total attenuated luminosity for both the galaxy and AGN components are listed in the top left. Assuming energy balance, this model, and models like it, predict significant FIR output where the the dust that is being heated by the intrinsically blue engine of the LRD, whether it is primarily driven by a starburst or an AGN.

Given that a reddened AGN is commonly invoked to model the red continuum of LRDs (e.g., Onoue et al. 2023; Labbé et al. 2023; Furtak et al. 2024; Wang et al. 2024a,b; Ma et al. 2024b, way more here), it stands to reason that the rising dust tori at $\sim 1\ \mu$m that typically accompany reddened quasars (e.g., Assef et al. 2016; Hamann et al. 2017; Ma et al. 2024a) would be seen in LRDs. However, to date, there has been essentially no detection of any significant hot dust in LRDs, even in stacks (Williams et al. 2024; Akins et al. 2024), outside of a potential small contribution at $\lambda_{\rm rest} \sim 6\mu$m in a z=2.26 system (Juodžbalis et al. 2024). RUBIES-BLAGN-1 already has mid-IR imaging in the MIRI F770W and F1800W filters ($\lambda_{\rm rest} \sim 1.5, 3.5\ \mu$m) from PRIMER (JWST-GO-1837), exhibiting very little evidence for a rising torus (Wang et al. 2024a). For our analysis, we utilize the fluxes reported in that work, 8.9 ± 0.4 and $13.0 \pm 0.6\ \mu$Jy in F770W and F1800W, respectively.

Observing setup here.

Text from Stacey about the reduction of the monster imaging here

Following Alberts et al. (2024), we measure the fluxes in our F1000W and F2100W using aperture sizes that enclose 65% of the energy of a point source (0.36" and 0.6", respectively), which we correct to total. Rather than using the pipeline uncertainty vector, we assume that the uncertainty in each pixel is equal to the standard deviation of the full image. The measured fluxes are 8.6 ± 0.3 and $9.0 \pm 0.9\ \mu$Jy in F1000W and F2100W, respectively.

2.2.2. *ALMA*

A little bit of background about the chosen bandpasses and sensitivity.

For both target LRDs, we carried out new ALMA observations in two bands in project 2024.1.00826.S. One band targeted the [CII] 158 μm line and underlying rest-frame $\approx$160 μm continuum emission, and the other band targeted the dust continuum emission at an observed frequency that depended on the redshift of each source. For A2744-45924, [CII] falls in the ALMA Band 7 receiver coverage at 347.82 GHz, and we also observed the continuum at $\sim$690 GHz in Band 9. For RUBIES-BLAGN-1, [CII] falls in ALMA Band 8 at 463.15 GHz, and we additionally observed the continuum at $\sim$240 GHz in Band 6. For the [CII] observations, the correlator was configured to provide $\approx$3.74 GHz of contiguous bandwidth around the [CII] sky frequency and 7.81 MHz channels; the alternate sideband used 31.25 MHz channels. The continuum-only observations of each target used the observatory-defined standard Band 9 or 6 continuum configurations.

Band 7 observations of A2744-45924 were executed on 2024 October 14 and 15 for a total on-source time of 97 min. The array consisted of 47 or 48 antennas on baselines spanning 15–500 m, producing a ≈0.7" synthesized beam with natural visibility weighting. The continuum sensitivity with this weighting is 14.4 μJy. We also produced [CII] cubes, which reach a sensitivity of 110 μJy in 100 $\mathrm{km\,s^{-1}}$ channels. The atmospheric transmission is smooth at the [CII] frequency, and we verified that the quoted depth scales as expected for narrower or wider velocity channels. The Band 9 observations were carried out on 2024 October 13 for a total on-source time of 99 min in excellent weather conditions. With natural weighting, the synthesized beam size was ≈0.3" with 110 μJy sensitivity. Concerned that this may resolve out any extended host galaxy emission, we also applied a 0.4" Gaussian uv taper; the resulting image has a ≈0.55" synthesized beam and 145 μJy sensitivity.

RUBIES-BLAGN-1 was observed in Band 8 on 2024 October 3 and 12 for a total of 198 min on-source with 47 and 44 antennas, respectively, and baselines ranging from 15–500 m. The synthesized beam with natural weighting is ∼0.45", but we again applied a uv taper to avoid resolving the target galaxy. The sensitivities below use a 0.5" to reach ∼0.75" angular resolution. The atmospheric transmission is more challenging at the observed Band 8 frequencies, with two main consequences. First, we discarded half of the continuum bandwidth in the upper sideband due to its proximity to a deep telluric oxygen feature (placing the continuum coverage in the lower sideband would have faced the same issue, but with the 448 GHz water line). The continuum sensitivity in the tapered image is 54 μJy. Second, the [CII] sky frequency is close to a narrow ozone line, resulting in ≈35% worse sensitivity in a 100 $\mathrm{km\,s^{-1}}$ bandwidth centered at $-30\,\mathrm{km\,s^{-1}}$. The consequence is that wider velocity channels include more data with better transmission; the naturally-weighted cubes reach sensitivities of 330, 170, and 125 μJy for 100, 300, and 500 $\mathrm{km\,s^{-1}}$ channels, respectively, at the expected [CII] frequency. Band 6 observations were carried out on 2024 October 18 and 19 for 115 min on-source. With natural visibility weighting, the synthesized beam is ≈1.0" and the data reach 7.0 μJy sensitivity.

2.2.3. *Herschel*

Finally, to constrain dust at rest-frame $sim20-40\mu$m, we utilize existing Herschel/PACs 100 and 160 μm imaging of our sources, which, in contrast with typical LRDs, are so luminous that these limits are relevant. For the BRD, we adopt the limits reported in (Wang et al. 2024a) from imaging obtained in the 3D-Herschel project (K. Whitaker et al. in prep). For A2744-45924, we utilize imaging from the Herschel Lensing Survey (Egami et al. 2010). We obtained reduced imaging products from the Herschel Science Archive and performed a 2D sky subtraction with SEP (Bertin & Arnouts 1996; Barbary 2016). We measure the flux and uncertainty in 4 and 6 arcsecond apertures at the source location and measure the total flux by multiplying by 2.5 and using the local RMS to estimate uncertainty (**Ivo, citation for this?**). We do not detect either image, and our 3σ upper limits are 1.7 mJy and 9.2 mJy at 100 and 160 μm respectively. **Do we need to think about confusion noise here?**

3. ANALYSIS

3.1. *Can typical galaxy/AGN dust explain IR observations of LRDs?*

- In the literature, essentially all models of LRDs assume that they are intrinsically blue and reddened. Under the assumption of energy balance, this energy must be re-radiated in the far-IR by the dust, which is heated by this radiation.

- While energy balance does not formally need to hold in any given object (as geometric considerations matter, we could be looking down the barrel of dust while the majority of the LRD light escapes unobscured perpendicular to our line of sight), the lack of FIR (or even MIR) detections in essentially all LRDs makes it unlikely that the covering fraction of LRDs is low and we are viewing them all under precisely the right configuration to see booming lines but no UV. **Save this for discussion?**

- In this section, we take energy balance considerations seriously, and ask the question of whether an LRD model can work under two assumptions: a "standard" (whether AGN or galaxy) dust SED or a hyper-tuned dust SED designed to allow the maximum LIR output.

- IR templates ingredients go here? Galaxy dust is a Draine et al. (2007) dust template with $U_{min} = 25$, $\gamma_e = 1$, and $q_{PAH} = 1$, the "physical" template corresponding to the hottest possible "cold" dust component ($\langle T_{\rm dust}\rangle$=45 K) with as little mid-IR contribution (from PAHs) as possible. **Change to skirtor**: AGN dust is a SKIRTOR (Stalevski et al. 2012, 2016) template that was selected to maximize energy output redward of 30 μm observed–

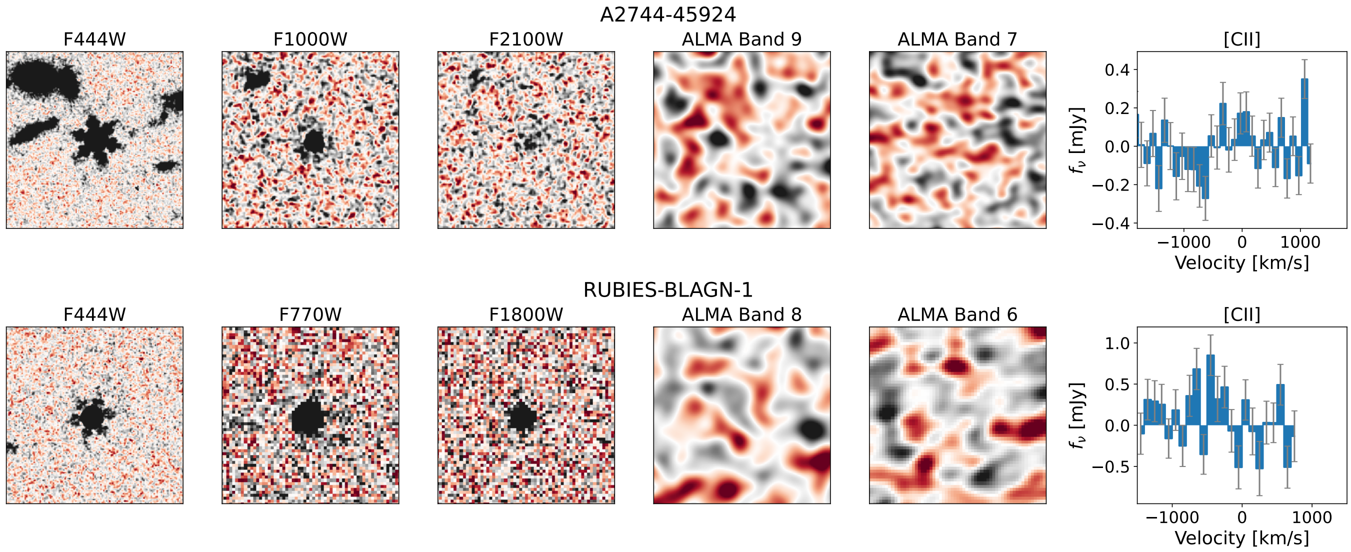

Figure 2. 6"x6" cutouts of A2744-45924 (top) and RUBIES-BLAGN-1 (bottom), showcasing the F444W imaging (A2744-45924: Bezanson et al. 2022; Weaver et al. 2024, RUBIES-BLAGN-1: JWST-GO-1837; PI Dunlop), as well as MIRI imaging (this program for A2744-45924, PRIMER for BRD-BLAGN-1), and new FIR continuum imaging and spectroscopy obtained with ALMA. Both sources are detected in the mid-IR but not in the far-IR. Additionally, neither source is significantly detected in [CII].

effectively, this is the coldest template in the library. **Might also add some of the Li et al. (2024) models.**

- Also a statement here that we adopt the LIR predictions from the models in Labbe et al. (2024) and Wang et al. (2024a) to scale these models, despite these models not being fit with FIR constraints (or MIR, in the case of Ivo). This is useful for evaluation whether the kinds of models that the entire field fits to these things

3.2. *Empirical Constraints on the IR Luminosity and Dust Temperature*

To do: shift the motivation a bit here to talk about how a big part of why we're doing this is because normal dust doesn't seem to work.

- The combination of the evidence of falling MIRI photometry, deep ALMA non-detections in the far-IR, and ancillary Herschel non-detections can empirically constrain the maximum energy output in the far-IR of these systems (e.g., Akins et al. 2024; Casey et al. 2024).

- In Figure 4, we demonstrate this for a range of temperatures by scaling modified blackbodies ($\beta = 2$) until they match or violate a constraint. In both A2744-45924 and RUBIES-BLAGN-1, the only place there is room for any considerable IR energy output ($\nu f_{\nu,\mathrm{IR}} > \nu f_{\nu,\mathrm{optical}}$) is at temperatures of ~ 200 K, where the Herschel upper limits kick in.

- In Figure 5, we formalize this by reporting the maximum $\log(L_{\mathrm{IR}}[L_\odot])$ as a function of the dust temperature, assuming no other contributions to the dust SED.

- This is not exactly the total maximum IR luminosity, as components that are far enough apart in temperature are ∼independent. However, because there is only a narrow band ($\sim 175-300$ K) where there is any room to hide any blackbodies with $L_{\mathrm{IR}} > 10^{12}\ L_\odot$, these constraints essentially do say that if there is any significant IR output, it must be coming out in a single component within that temperature range.

- We annotate this figure with the energy balance predictions from the models in Labbe et al. (2024) and Wang et al. (2024a), again making the point that, if the intrinsic SEDs really look like a typical starburst or AGN, there is essentially no room to hide this luminosity even with as narrow an IR SED as you can imagine.

4. DISCUSSION AND CONCLUSIONS

There are basically three possibilities here:

4.1. *Geometry*

- Little Red Dots are actually this dusty, but the geometric configuration is such that a huge chunk

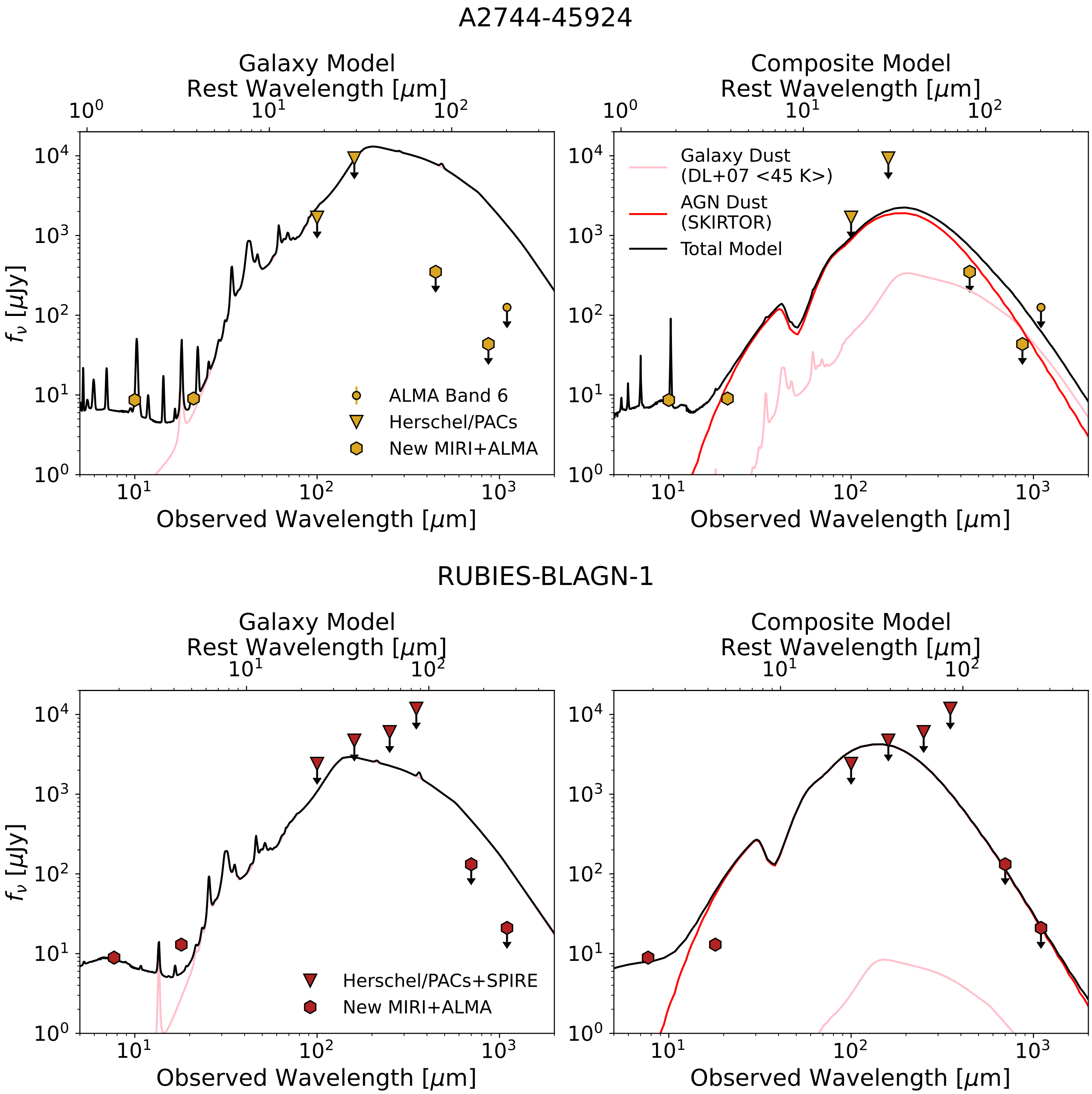

Figure 3. The IR spectral energy distributions of A2744-45924 (top) and RUBIES-BLAGN-1 (bottom). Existing NIRCAM photometry (and ALMA Band 6 data in the case of A2744-45924) are shown as circles. Herschel PACs and SPIRE upper limits are shown as triangles. New MIRI and ALMA limits are shown as hexagons. In the first row, we show the predictions for the IR SED using the galaxy-only fits from Labbe et al. (2024) and Wang et al. (2024a), assuming the dust emits as a $\langle T_{\rm dust} \rangle = 45$ K Draine et al. (2007) template scaled to the attenuated luminosity (pink). On the right, we show the composite models from the same work, with the attenuated luminosity of the galaxy component emitted in the same Draine et al. (2007) template and the attenuated AGN emitted with the coldest SKIRTOR model (red). In all cases, the total model is shown in black and is incapable of being fully consistent with our new constraints.

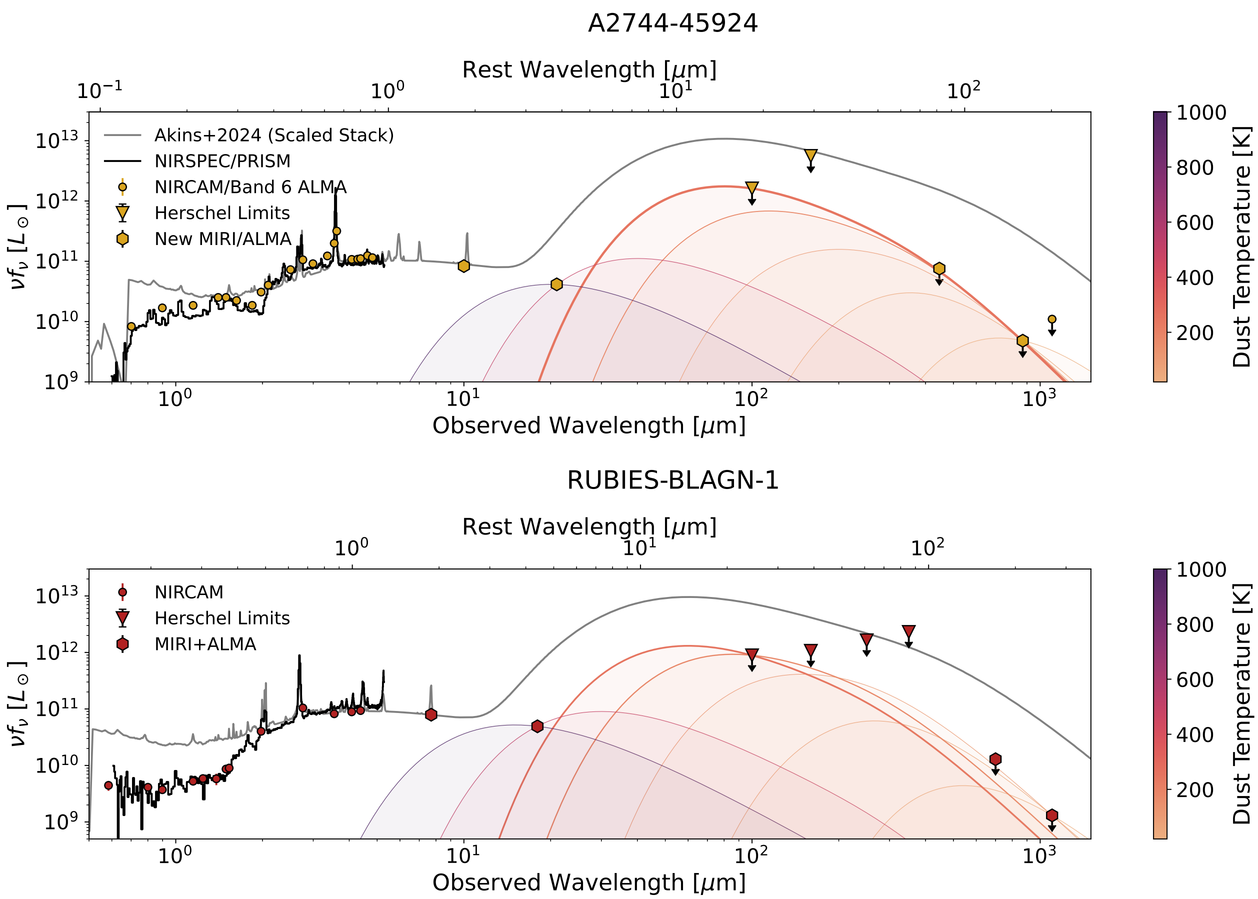

Figure 4. (Top): The full SEDs for A2744-45924 (top) and RUBIES-BLAGN-1 (bottom) containing all existing optical-FIR data, with existing NIRCAM photometry shown as circles and NIRCam spectra shown in black. Herschel PACs and SPIRE upper limits are shown as triangles. New MIRI and ALMA limits are shown as hexagons. The colored curves indicate the maximum contribution of a single temperature T= 20, 50, 100, 175, 250, 500, and 1000 K modified blackbody ($\beta = 2$), subject to the new IR constraints. The line width of each blackbody is proportional to its luminosity. The non-detection of any rising dust at rest-frame 4 μm essentially rules out any significant luminosity contribution from hot ($T > 500$ K) dust. Similarly, the ALMA non-detections rule out any significant contribution from cold ($T < 50$ K) dust. Herschel non-detections place a ceiling of $\sim 10^{12}$ $L_\odot$ in a warm component at $T \sim 250$ K. Also shown is the stacked maximal LRD SED from Akins et al. (2024) (grey), scaled to the rest-optical luminosity of our sources, illustrating that our observations allow for a much narrower range of $L_{\rm optical}/L_{\rm IR}$ than their limits. **To do for David: Improve colors per Rachel's suggestions, unify with a single colorbar?**

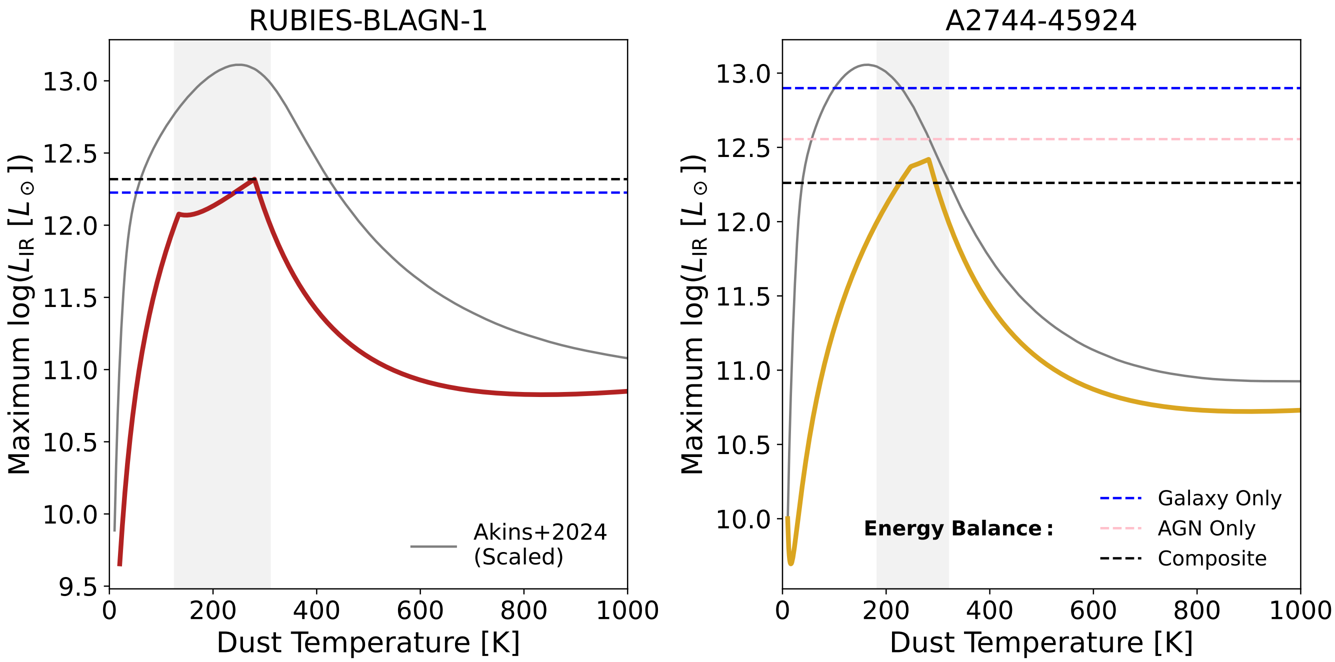

Figure 5. The maximum IR that can be contained in a single blackbody for RUBIES-BL-AGN-1 (left) and A2744-45924 (right), measured by scaling blackbodies at a given temperature until they violate a detection (in the case of MIRI) or a 3σ upper limit (in the case of Herschel and ALMA). Also shown are the Akins et al. (2024) constraints (grey), which we measure from their upper limit SED after scaling to the luminosity of our sources. There is a narrow band of temperature at ∼90-250 K where any appreciable IR energy ($L > 10^{12} L_\odot$, shaded region) can be output; in both sources, the presence of hotter and colder luminous dust components is ruled out by MIRI and ALMA limits respectively. In addition, for each LRD, we also show as dashed lines the attenuated luminosity predictions for galaxy-only (blue), AGN-only (pink), and galaxy+AGN composite (black) models from Wang et al. (2024a) and Labbe et al. (2024). **TBD: In both cases**, there is essentially no room to hide the FIR output of a highly attenuated starburst or AGN, and even composite models with the most flexibility to produce the red continuum with intrinsically red light can barely avoid being ruled out.

of the energy escapes through unobscured sightlines. This would allow for lower dust luminosities without requiring a fundamental modification to any of the LRD models people are fitting

- This is unlikely to be true. Such a model predicts that we *would* see the analogous blue things that don't have these sight lines, and LRDs are just too numerous relative to e.g., quasars or massive galaxies for that to be the case.

4.2. *LRDs just have very strange dust SEDs that are unlike anything we've ever seen*

- We can't rule this out, but on the flip side, it seems like a huge conspiracy that all the energy in these things, regardless of redshift, is coming out in a hyper specific band of temperature, with no corresponding hot or cold tail
- Even in this case, the energy balance solutions for these two objects are getting dangerously close to violating these limits even if we hide all the luminosity in that single peak. Dusty starburst is totally out, obscured Temple-like AGN is barely hanging on, but composite models are ∼correct and we just need to go a bit deeper in the FIR and we'll see the dust we expect to see
- This just feels unlikely. What are the super specific gas and dust properties of LRDs where this occurs? Why do we not detected appreciable [CII] emission if there's any galaxy population–surely these things aren't all totally quenched at the time of observation but still host to a significant massive population?

4.3. *LRDs are not actually all that dusty–they're intrinsically red*

- This is really looking like the most likely option.
- There's still the issue of how you ionize the lines–collisional ionization?–but it's just getting to be very hard to square an intrinsically blue SED with the observed red SED in the optical and the lack of real FIR energy output

- What could this be? Something Inayoshi & Maiolino (2024) like with what's basically a super-star atmosphere surrounding the AGN seems promising for producing the n=2 absorption. But in the Ji+2025 implementation, they still needed significant dust to make it work, and it honestly doesn't seem that different than our composite model here.

- Hard to look at the way the red end is starting to turn over in νf_ν and think that it's going to keep rising...

4.4. *Where do we go from here?*

- Lower-z/higher-z sources that are comparably luminous to these two will give us the best chance at digging deeper at the mid-/far-IR respectively. So we can look for those and do some deep dives similar to this.

- If we do that and still continue to not find any evidence of a real dust SED, it's probably time to really get serious about the ingredients that we are using to model these systems just fundamentally not being right.

- We probably shouldn't continue just fitting standard SED/AGN fitting codes to photometric samples and then making conclusions based on the results of those fits.

Support for this work was provided by The Brinson Foundation through a Brinson Prize Fellowship grant.

REFERENCES

Akins, H. B., Casey, C. M., Lambrides, E., et al. 2024, arXiv e-prints, arXiv:2406.10341, doi: 10.48550/arXiv.2406.10341

Alberts, S., Lyu, J., Shivaei, I., et al. 2024, ApJ, 976, 224, doi: 10.3847/1538-4357/ad7396

Assef, R. J., Walton, D. J., Brightman, M., et al. 2016, ApJ, 819, 111, doi: 10.3847/0004-637X/819/2/111

Baggen, J. F. W., van Dokkum, P., Labbé, I., et al. 2023, ApJL, 955, L12, doi: 10.3847/2041-8213/acf5ef

Baggen, J. F. W., van Dokkum, P., Brammer, G., et al. 2024, arXiv e-prints, arXiv:2408.07745, doi: 10.48550/arXiv.2408.07745

Barbary, K. 2016, Journal of Open Source Software, 1, 58, doi: 10.21105/joss.00058

Bertin, E., & Arnouts, S. 1996, A&AS, 117, 393, doi: 10.1051/aas:1996164

Bezanson, R., Labbe, I., Whitaker, K. E., et al. 2022, arXiv e-prints, arXiv:2212.04026, doi: 10.48550/arXiv.2212.04026

Casey, C. M., Akins, H. B., Kokorev, V., et al. 2024, ApJL, 975, L4, doi: 10.3847/2041-8213/ad7ba7

Draine, B. T., Dale, D. A., Bendo, G., et al. 2007, ApJ, 663, 866, doi: 10.1086/518306

Egami, E., Rex, M., Rawle, T. D., et al. 2010, A&A, 518, L12, doi: 10.1051/0004-6361/201014696

Furtak, L. J., Labbé, I., Zitrin, A., et al. 2024, Nature, 628, 57, doi: 10.1038/s41586-024-07184-8

Hamann, F., Zakamska, N. L., Ross, N., et al. 2017, MNRAS, 464, 3431, doi: 10.1093/mnras/stw2387

Inayoshi, K., & Maiolino, R. 2024, arXiv e-prints, arXiv:2409.07805, doi: 10.48550/arXiv.2409.07805

Ji, X., Maiolino, R., Übler, H., et al. 2025, arXiv e-prints, arXiv:2501.13082, doi: 10.48550/arXiv.2501.13082

Juodžbalis, I., Ji, X., Maiolino, R., et al. 2024, MNRAS, doi: 10.1093/mnras/stae2367

Labbé, I., Greene, J. E., Bezanson, R., et al. 2023, arXiv e-prints, arXiv:2306.07320, doi: 10.48550/arXiv.2306.07320

Labbe, I., Greene, J. E., Matthee, J., et al. 2024, arXiv e-prints, arXiv:2412.04557, doi: 10.48550/arXiv.2412.04557

Li, Z., Inayoshi, K., Chen, K., Ichikawa, K., & Ho, L. C. 2024, arXiv e-prints, arXiv:2407.10760, doi: 10.48550/arXiv.2407.10760

Ma, Y., Goulding, A., Greene, J. E., et al. 2024a, ApJ, 974, 225, doi: 10.3847/1538-4357/ad710c

Ma, Y., Greene, J. E., Setton, D. J., et al. 2024b, arXiv e-prints, arXiv:2410.06257, doi: 10.48550/arXiv.2410.06257

Onoue, M., Inayoshi, K., Ding, X., et al. 2023, ApJL, 942, L17, doi: 10.3847/2041-8213/aca9d3

Stalevski, M., Fritz, J., Baes, M., Nakos, T., & Popović, L. Č. 2012, MNRAS, 420, 2756, doi: 10.1111/j.1365-2966.2011.19775.x

Stalevski, M., Ricci, C., Ueda, Y., et al. 2016, MNRAS, 458, 2288, doi: 10.1093/mnras/stw444

Wang, B., de Graaff, A., Davies, R. L., et al. 2024a, arXiv e-prints, arXiv:2403.02304, doi: 10.48550/arXiv.2403.02304

Wang, B., Leja, J., de Graaff, A., et al. 2024b, ApJL, 969, L13, doi: 10.3847/2041-8213/ad55f7

Weaver, J. R., Cutler, S. E., Pan, R., et al. 2024, ApJS, 270, 7, doi: 10.3847/1538-4365/ad07e0

Williams, C. C., Alberts, S., Ji, Z., et al. 2024, ApJ, 968, 34, doi: 10.3847/1538-4357/ad3f17